# Anomalous Excitation Spectra of Frustrated Quantum Antiferromagnets

Weihong Zheng,[1] John O. Fjærestad,[2] Rajiv R. P. Singh,[3] Ross H. McKenzie,[2] and Radu Coldea[4]

[1]*School of Physics, The University of New South Wales, Sydney, NSW 2052, Australia*
[2]*Department of Physics, The University of Queensland, Brisbane, QLD 4072, Australia*
[3]*Department of Physics, University of California, Davis, California 95616, USA*
[4]*Department of Physics, University of Oxford, Oxford OX1 3PU, United Kingdom*

We use series expansions to study the excitation spectra of spin-$1/2$ antiferromagnets on anisotropic triangular lattices. For the isotropic triangular lattice model (TLM), the high-energy spectra show several anomalous features that differ strongly from linear spin-wave theory (LSWT). Even in the Néel phase, the deviations from LSWT increase sharply with frustration, leading to rotonlike minima at special wave vectors. We argue that these results can be interpreted naturally in a spinon language and provide an explanation for the previously observed anomalous finite-temperature properties of the TLM. In the coupled-chains limit, quantum renormalizations strongly enhance the one-dimensionality of the spectra, in agreement with experiments on $Cs_2CuCl_4$.

One of the central problems in quantum magnetism is understanding the properties of two-dimensional (2D) spin-$1/2$ Heisenberg antiferromagnets (HAFM's). A question of particular interest is whether the interplay between quantum fluctuations and geometrical frustration can lead to unconventional ground states and/or excitations. Candidate materials which have recently attracted much attention include $Cs_2CuCl_4$ [1] and $\kappa$-$(BEDT\text{-}TTF)_2Cu_2(CN)_3$ [2].

If the ground state is magnetically ordered, the system must have gapless magnon excitations, which at sufficiently low energies are expected to be well described by semiclassical (i.e., large-$S$) approaches such as spin-wave theory (SWT) and the nonlinear sigma model (NLSM). However, if the magnon dispersion at higher energies deviates significantly from the semiclassical predictions, it is possible that the proper description of the excitations, valid at all energies, is in terms of pairs of $S = 1/2$ spinons. In this unconventional scenario, the magnon is a *bound* state of two spinons, lying below the two-spinon (particle-hole) continuum.

In this Letter, we use series expansions to calculate the magnon dispersion of 2D frustrated $S = 1/2$ HAFM's. Our main finding is that for the triangular lattice model (TLM) the dispersion shows major deviations from linear SWT (LSWT) at high energies (Fig. 1). We argue that these deviations can be qualitatively understood in terms of a two-spinon picture [3], provided the spinon dispersion has minima at $K_i/2$, where $K_i$ is a magnetic Bragg vector. Based on this interpretation of the TLM spectra, we propose an explanation for the anomalous finite-temperature behavior found in high-temperature series expansion studies [4].

Both qualitatively and quantitatively, the deviations from LSWT found here for the TLM are much more pronounced than those previously reported [5–8] for the

high-energy spectra of the square lattice model (SLM). We point out that the deviations from SWT increase in the Néel phase, too, upon adding frustration to the SLM. We further consider the limit of our model relevant to $Cs_2CuCl_4$ and show that the calculated excitation spectra are in good agreement with experiments [1].

*Model.*—We consider a $S = 1/2$ HAFM on an anisotropic triangular lattice, with exchange couplings $J_1$ and $J_2$ [Fig. 2(a)]. This model interpolates among the SLM ($J_1 = 0$), TLM ($J_1 = J_2$), and decoupled chains ($J_2 = 0$). Classically, the model has Néel order for $J_1 \leq J_2/2$ with $q = \pi$ and helical order for $J_1 > J_2/2$ with $q = \arccos(-J_2/2J_1)$, where $q$ ($2q$) is the angle between
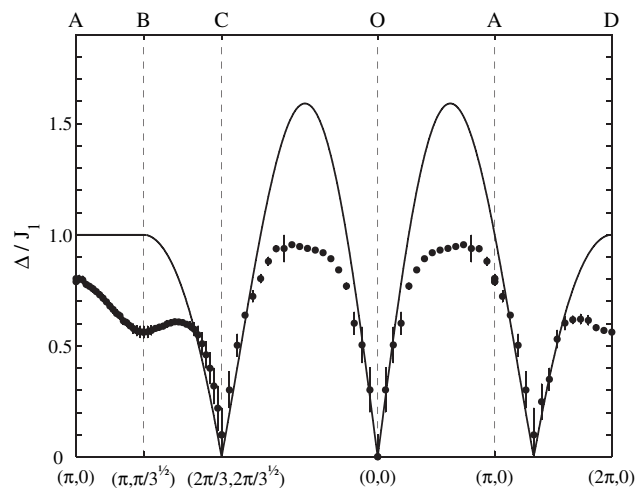


FIG. 1. Excitation spectrum for the TLM ($J_1 = J_2$) along the path ABCOAQD shown in Fig. 4. The high-energy spectrum is strongly renormalized downwards compared to the LSWT prediction (solid line). Note the roton minima at B and D and the flat dispersion in the middle parts of CO and OQ.
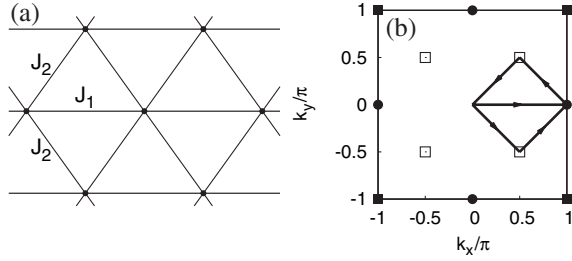
FIG. 2. (a) Exchange constants $J_1$ and $J_2$ for the $S = 1/2$ HAFM on the anisotropic triangular lattice. The model can also be viewed as a square lattice with an extra exchange along one diagonal. (b) Brillouin zone for the frustrated SLM, in standard square lattice notation (the frustrating $J_1$ bonds are taken to lie along the $+45°$ directions in real space). The excitation spectra in Fig. 3 are plotted along the bold path. Also shown are the locations of the Bragg vectors (solid squares) and the local roton minima (solid circles) in the $S = 1$ dispersion and the global minima of the $S = 1/2$ spinon dispersion (open squares) in the Néel phase. Note that the 90° rotation invariance present for $J_1 = 0$ is lost for $J_1 > 0$.

nearest-neighbor spins along $J_2$ ($J_1$). The phase diagram for $S = 1/2$ was studied in Refs. [9,10].

*Series expansion method.*—In order to develop series expansions for the helical phase (see Ref. [9] for expansions for the Néel phase spectra), we assume that the spins order in the $xz$ plane, with nearest-neighbor angles $q$ and $2q$ as defined above; $q$ (generally different from the classical result) is determined by minimizing the ground state energy. We now rotate all the spins, so as to make the ordered state ferromagnetic, and introduce an anisotropy parameter in the Hamiltonian $H(\lambda) = H_0 + \lambda V$, so that $H(0)$ is a ferromagnetic Ising model and $H(1)$ is the spin-rotation invariant Heisenberg model [9]. We use linked-cluster methods to develop series expansions in powers of $\lambda$ for ground state properties and the triplet excitation spectra. The calculation of the spectra is particularly challenging as $S^z$ is not conserved. Because of single-spin flip terms in $V$, the one-magnon state and the ground state belong to the same sector, and the linked-cluster expansion with the traditional similarity transformation [11] fails. To get a successful linked-cluster expansion, one has to use a multiblock orthogonality transformation [12]. We have computed the series for ground state properties to order $\lambda^{11}$ and for the spectra to order $\lambda^9$ for $J_1 = J_2$ and to order $\lambda^8$ otherwise. The properties for $\lambda = 1$, discussed in the following, are obtained from standard series extrapolation methods.

*Square lattice model.*—Several numerical studies [5–8] have reported deviations from SWT for high-energy excitations in the SLM. While 1st order SWT (i.e., LSWT) and 2nd order SWT predict no dispersion along $(\pi − x, x)$, 3rd order SWT finds a weak dispersion, with the energy at $(\pi, 0)$ ~2% lower than at $(\pi/2, \pi/2)$ [8,13,14]. In contrast, the most recent quantum Monte Carlo (QMC) [7] and

series expansion [8] studies find the energy at $(\pi, 0)$ to be ~9% lower. These deviations from SWT have been interpreted [6,15,16] in terms of a resonating valence-bond (RVB) picture, in which the ground state is described as a $\pi$-flux phase [17] modified by correlations producing long-range Néel order [15], and the Goldstone modes (magnons) are bound states of a particle and a hole spinon [15,16]. The magnon dispersion, calculated using a random phase approximation (RPA), has local minima at $(\pi, 0)$ [15,16] (in qualitative agreement with the series or QMC results), the locations of which are intimately related to the fact that the spinon dispersion has minima at $(\pi/2, \pi/2)$ [15,17].

*Frustrated square lattice model.*—The Néel phase persists up to $J_1/J_2 = (J_1/J_2)_c \gtrsim 0.7$, after which the system enters a dimerized phase [9]. As the frustration $J_1/J_2$ is increased towards $(J_1/J_2)_c$, the local minimum at $(\pi, 0)$ becomes more pronounced (see Fig. 3); for $J_1/J_2 = 0.7$, the energy difference between $(\pi/2, \pi/2)$ and $(\pi, 0)$ has increased to ~31%. In contrast, LSWT predicts no energy difference [18]. These results lend further support to the RVB/flux-phase picture. The locations of the Bragg vectors, roton minima, and spinon minima in the Néel phase are shown in Fig. 2(b).

*Triangular lattice model.*—Next, we consider the TLM ($J_1 = J_2$), whose ground state has 120° ordering between neighboring spins [19]. Figure 1 shows the excitation spectrum plotted along the path ABCOQD in Fig. 4. While the low-energy spectrum near the (magnetic) Bragg vectors looks conventional, the high-energy part of the excitation spectrum shows several anomalous features which both qualitatively and quantitatively differ strongly from LSWT: (i) At high energies, the spectrum is renor-
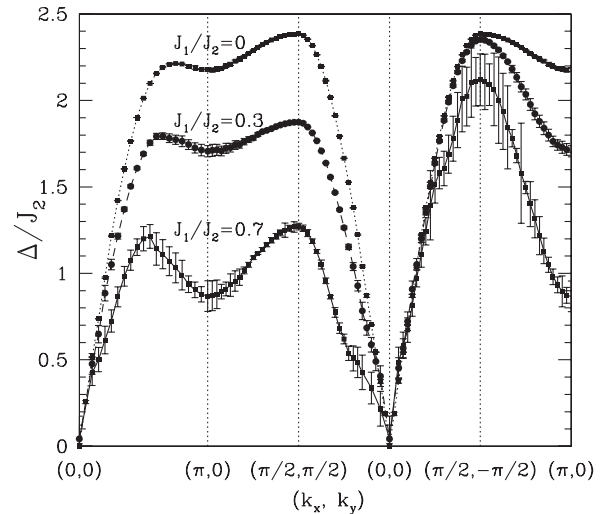


FIG. 3. Excitation spectra in the Néel phase. As $J_1/J_2$ is increased, the local roton minimum at $(\pi, 0)$ becomes more pronounced, and the energy difference between $(\pi, 0)$ and $(\pi/2, \pi/2)$, which LSWT predicts to be zero, increases.
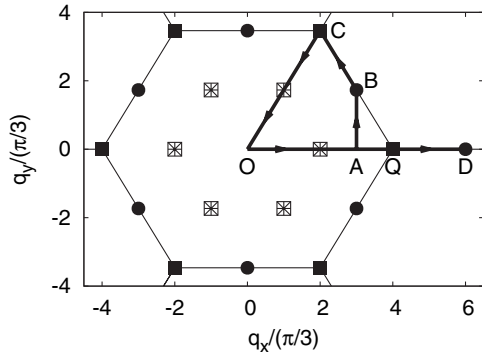
FIG. 4.   Brillouin zone diagram for the TLM. Bragg vectors (solid squares), local roton minima (solid circles), and midpoints of flat dispersion regions (stars) for the spin-1 dispersion are shown, as well as the global minima of the proposed $S = 1/2$ spinon dispersion (open squares). Note that the latter two sets of wave vectors coincide. The excitation spectra in Figs. 1 and 5 are plotted along the path ABCOAD.

malized downwards with respect to LSWT. (ii) The excitation spectrum is very flat in the region halfway between the origin and a Bragg vector, with the midpoint renormalized downwards with respect to LSWT by ~40%. (iii) There are local, rotonlike, minima at the midpoints of the Brillouin zone edges, whose energy is ~44% lower than the LSWT prediction. These strong downward renormalizations for the TLM should be contrasted with the SLM, for which quantum fluctuations always renormalize the LSWT spectrum *upwards* and by amounts never exceeding 20%.

*Two-spinon interpretation.*—We will argue that these results for the TLM are suggestive of spinons in the model. Our basic hypothesis is that an "uncorrelated" RPA-like calculation for the TLM, analogous to that discussed in Ref. [20] for the SLM, should produce a spectrum similar to the LSWT result, but it will be modified by correlations [21]. In particular, repulsion from the two-spinon (particle-hole) continuum can lower the magnon energy, especially at wave vectors where this continuum has minima. These minima should occur at $(K_i - K_j)/2$ corresponding to the creation of minimum-energy particle-hole excitations with particle and hole wave vectors $K_i/2$ and $K_j/2$, respectively, the locations of which are shown in Fig. 4 (the $K_i$ are magnetic Bragg vectors). This equals (see Fig. 4) a "roton" wave vector, when $K_i$ and $K_j$ differ by a $2\pi/3$ rotation around the origin, and a wave vector at a spinon minimum, if $K_i$ and $K_j$ differ by a $\pi/3$ rotation. Figure 1 shows that, at both types of wave vectors, the excitation spectrum is strongly renormalized downwards with respect to the LSWT. At the former (latter) type of wave vector, the LSWT dispersion is flat (peaked), which upon renormalization leads to a dip (flat region) in the true spectrum. Thus, we attribute these deviations to the existence of a two-spinon continuum.

For the SLM, the spectral weight of the magnon peak at $(\pi, 0)$ is considerably smaller than at $(\pi/2, \pi/2)$ (60% vs 85%) [7], and the magnon energy deviates much more from SWT at $(\pi, 0)$ than at $(\pi/2, \pi/2)$. This suggests quite generally that the relative weight of the magnon peak decreases with increasing deviation between the true magnon energy and the LSWT prediction. Therefore, one might expect the contribution of the two-spinon continuum to be considerably larger for the TLM than for the SLM.

As for the spinons proposed for the SLM [15–17], the locations of the minima in the spinon dispersion reflect a *d*-wave character of the underlying RVB pairing correlations. A *d*-wave RVB state of this type, but without long-range order, was discussed for the TLM in Ref. [22]. Its energy was, however, notably higher than that of the ordered ground state, and attempts to modify this RVB state to incorporate long-range order were not successful. A mean-field RVB state for the TLM with *bosonic* spinons, whose dispersion has minima close to $K_i/2$, was considered in Refs. [23,24], again without long-range order. In light of our spinon hypothesis for the TLM, it would clearly be of interest to revisit these problems.

*Explanation of finite-temperature anomalies.*—The existence of roton minima and their description in terms of pairs of spinons provide a possible explanation for the sharply different temperature dependent properties of the SLM and TLM. For the SLM, the temperature dependence of the correlation length is consistent with a NLSM description in the renormalized classical (RC) regime over a considerable temperature range [25]. Even though the ground state moment and spin stiffness are comparable in the two models, for the TLM the correlation length was found to be orders of magnitude smaller at $T = J/4$ with a spin stiffness decreasing with decreasing temperature (and longer length scales) [4], inconsistent with the NLSM description in the RC regime [26]. We suggest that these differences are due to the fact that (see Figs. 1 and 3) the spinon gap $E_s$ (which is half the roton energy) is 4 times smaller for the TLM than for the SLM (0.28$J$ versus 1.1$J$). Substantial thermal excitation of spinons for temperatures comparable to $E_s$ will make a significant contribution to the entropy and reduce the spin stiffness. Following an argument by Ng [27], we expect that thermal excitation of spinons will cause a NLSM description to break down when $T \sim E_s$. The results of the high-temperature expansions for both models are consistent with this estimate [4].

$J_1/J_2 = 3$ *and* $Cs_2CuCl_4$.—The ratio $J_1/J_2 = 3$, closer to the decoupled chains limit, is relevant for $Cs_2CuCl_4$, which has an extremely rich excitation spectrum [1] with well-defined spin waves at low energies below the Néel temperature $T_N$, and a continuum, strongly reminiscent of the two-spinon continuum in one-dimensional (1D) antiferromagnets, which persists well above $T_N$. Compared to LSWT, the series dispersion (Fig. 5) is enhanced by ~53% along the chains (close to the value for 1D chains) and
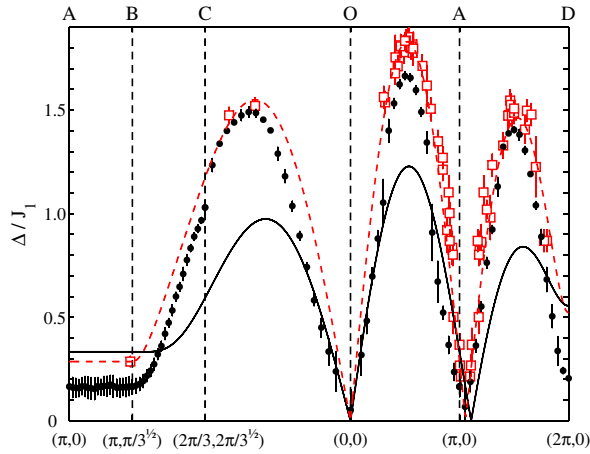
FIG. 5 (color online).   Excitation spectrum for $J_1/J_2 = 3$ (solid points from series) along the path ABCOAD in Fig. 4, compared to experimental dispersion in $Cs_2CuCl_4$ (squares from Ref. [1]; dashed line is the experimental fit), where the exchange ratio is similar, $J_2/J_1 = 0.34(3)$ and $J_2 = 0.128(5)$ meV. Compared to LSWT for $J_1/J_2 = 3$ (solid line), these spectra are enhanced along the $J_1$ bonds and decreased perpendicular to them.

reduced by $\sim 50\%$ perpendicular to the chains. [In contrast, higher order SWT [28] gives only weak enhancement ($\sim 13\%$) over LSWT along the chains.] Thus, quantum fluctuations make the system appear much more 1D. Overall, the series dispersion agrees well with the experimental dispersion for $Cs_2CuCl_4$, also shown in Fig. 5, whose enhancement and reduction factors (derived using a slightly different $J_1/J_2$ ratio; see caption) are $\sim 63\%$ and $\sim 17\%$. The large difference between the theoretical and experimental reduction factors perpendicular to the chains may be due to the Dzyaloshinski-Moriya interaction in $Cs_2CuCl_4$ (not included in the series calculations), which may make the system less 1D (it has the same path as $J_2$ and a coupling constant $\sim 0.15 J_2$) [28].

[1] R. Coldea *et al.*, Phys. Rev. B **68**, 134424 (2003).
[2] Y. Shimizu *et al.*, Phys. Rev. Lett. **91**, 107001 (2003).
[3] P. W. Anderson, Mater. Res. Bull. **8**, 153 (1973); P. Fazekas and P. W. Anderson, Philos. Mag. **30**, 423 (1974); P. W. Anderson, Science **235**, 1196 (1987).
[4] N. Elstner *et al.*, Phys. Rev. Lett. **71**, 1629 (1993); J. Appl. Phys. **75**, 5943 (1994).
[5] R. R. P. Singh and M. P. Gelfand, Phys. Rev. B **52**, R15 695 (1995).
[6] O. F. Syljuåsen and H. M. Rønnow, J. Phys. Condens. Matter **12**, L405 (2000).
[7] A. W. Sandvik and R. R. P. Singh, Phys. Rev. Lett. **86**, 528 (2001).
[8] W. Zheng *et al.*, Phys. Rev. B **71**, 184440 (2005).
[9] Z. Weihong *et al.*, Phys. Rev. B **59**, 14 367 (1999).
[10] C. H. Chung *et al.*, J. Phys. Condens. Matter **13**, 5159 (2001).
[11] M. P. Gelfand, Solid State Commun. **98**, 11 (1996).
[12] W. Zheng *et al.*, Phys. Rev. B **63**, 144410 (2001).
[13] Z. Weihong and C. J. Hamer, Phys. Rev. B **47**, 7961 (1993).
[14] J. Igarashi and T. Nagao, Phys. Rev. B **72**, 014403 (2005).
[15] T. C. Hsu, Phys. Rev. B **41**, 11 379 (1990).
[16] C. M. Ho *et al.*, Phys. Rev. Lett. **86**, 1626 (2001).
[17] I. Affleck and J. B. Marston, Phys. Rev. B **37**, R3774 (1988).
[18] J. Merino *et al.*, J. Phys. Condens. Matter **11**, 2965 (1999).
[19] B. Bernu *et al.*, Phys. Rev. B **50**, 10 048 (1994); R. R. P. Singh and D. A. Huse, Phys. Rev. Lett. **68**, 1766 (1992); D. J. J. Farnell *et al.*, Phys. Rev. B **63**, 220402(R) (2001); L. Capriotti *et al.*, Phys. Rev. Lett. **82**, 3899 (1999).
[20] J. R. Schrieffer *et al.*, Phys. Rev. B **39**, 11 663 (1989).
[21] See also discussions of Eq. (2.44) and Fig. 2 in Ref. [15].
[22] T. K. Lee and S. Feng, Phys. Rev. B **41**, 11 110 (1990).
[23] D. Yoshioka and J. Miyazaki, J. Phys. Soc. Jpn. **60**, 614 (1991).
[24] K. Lefmann and P. Hedegård, Phys. Rev. B **50**, 1074 (1994).
[25] S. Chakravarty *et al.*, Phys. Rev. B **39**, 2344 (1989).
[26] P. Azaria *et al.*, Phys. Rev. Lett. **68**, 1762 (1992); A. V. Chubukov *et al.*, Phys. Rev. Lett. **72**, 2089 (1994).
[27] T. K. Ng, Phys. Rev. Lett. **82**, 3504 (1999).
[28] M. Y. Veillette *et al.*, Phys. Rev. B **72**, 134429 (2005).